Isospin dependence of nuclear multifragmentation in statistical model*

ZHANG Lei(张蕾)[1;1)] XIE Dong-Zhu(谢东珠)[2] ZHANG Yan-Ping(张艳萍)[3] GAO Yuan(高远)[1]

[1] School of Information Engineering, Hangzhou Dianzi University, Hangzhou 310018, China
[2] College of Mathematics and Sciences, Shanghai Normal University, Shanghai 200234, China
[3] Department of Nuclear Physics, China Institute of Atomic Energy, Beijing 102413, China

Abstract: The evolution of nuclear disintegration mechanisms with increasing excitation energy, from compound nucleus to multifragmentation, has been studied by using the Statistical Multifragmentation Model (SMM) within a micro-canonical ensemble. We discuss the observable characteristics as functions of excitation energy in multifragmentation, concentrating on the isospin dependence of the model in its decaying mechanism and break-up fragment configuration by comparing the $A_0 = 200$, $Z_0 = 78$ and $A_0 = 200$, $Z_0 = 100$ systems. The calculations indicate that the neutron-rich system ($Z_0 = 78$) translates to a fission-like process from evaporation later than the symmetric nucleus at a lower excitation energy, but gets a larger average multiplicity as the excitation energy increases above 1.0 MeV/u.

Key words: statistical model, multifragmentation, microcanonical ensemble, isospin dependence

PACS: 21.65.-f, 24.10.Pa, 25.70.Pq **DOI:** 10.1088/1674-1137/35/6/011

1 Introduction

Many models have been developed to describe the breakup of a large nucleus subjected to excitation energies greater than a few MeV per nucleon, a process known as nuclear multifragmentation [1–9]. This phenomenon has drawn much attention because of the possibility of observing a liquid-gas phase transition in nuclear matter [10–12]. Many approaches have been proposed to describe different aspects of the nuclear multifragmentation process [13]. Among them, the Statistical Multifragmentation Model (SMM) presented in Refs. [14–21], which is called the Copenhagen model, has been largely used for interpreting experimental data about multiple fragment production in different nuclear reactions [22–30].

Compared with the dynamical models, statistical treatments do not describe the whole collision process. Instead, it is the configuration of the system after the most violent stages of the reaction that are considered, from which one can predict the properties of the fragment production. In the framework of the statistical model, as a result of the most violent stages of the collision, the excited nuclear system is assumed thermally equilibrated and breaks up simultaneously as it cools down. The different fragmentation modes are weighed according to their statistical factors, which depend on the statistical ensemble adopted [1, 9, 14], and all of the statistical approaches are very successful in quantitatively describing many features of nuclear multifragmentation [1, 23].

In this work, we compare the thermodynamic quantities of different systems predicted by the SMM based on its microcanonical versions [14–16], by concentrating on the isospin dependence of the model. The calculation of physical observables, such as the average multiplicity and temperature of the model as a function of excitation energy, are discussed, and the mass distributions at different excitation energies are also demonstrated. In particular, the isospin effect on the multifragmentation mechanism and the fragment configuration are very well investigated.

In Sec. 2, we give a detailed framework of the SMM within a microcanonical ensemble used in the

Received 25 October 2010

∗ Supported by Natural Science Foundation of China (10975064, 10905041, 11005171) and General Programs of Social Science Research Fund of Ministry of Education of China (10YJAZH137)

1) E-mail: zhanglei@hdu.edu.cn

calculations. The comparison among their predictions is discussed in Sec. 3. We conclude in Sec. 4 with a brief summary of the multifragmentation process and fragment configuration.

2 The statistical multifragmentation model

In the SMM, the main physical picture is described where a hot and compressed source is formed at the late stages of the reaction. This excited source then undergoes a simultaneous statistical breakup. In this section, we present the microcanonical ensemble versions of the model used in this work [14–16].

In the microcanonical version, each fragmentation mode f of an excited source with mass and atomic numbers A_0 and Z_0, respectively, must strictly be consistent with the mass, charge and energy conservation, and thus the following constraints are imposed for each partition,

$$A_0 = \sum_{A,Z} N_{A,Z} A\,, \tag{1}$$

$$Z_0 = \sum_{A,Z} N_{A,Z} Z\,, \tag{2}$$

and

$$-B_{A_0,Z_0} + E^* = \frac{3}{5}\frac{Z_0^2 e^2}{R} + \sum_{A,Z} N_{A,Z} E_{A,Z}(T), \tag{3}$$

where $N_{A,Z}$ represents, within a fragmentation mode f, the multiplicity of a fragment with mass and atomic numbers A and Z; B_{A_0,Z_0} stands for the binding energy of the source [31]; and E^* represents its excitation energy at temperature T. The total energy on the right hand side of the equation is written as the sum of the Coulomb energy and the contribution of each fragment $E_{A,Z}(T)$ [32]. The latter is calculated using a liquid drop parametrization of the fragment's energy and has the following contributions [16],

$$E_{A,Z}(T) = -B_{A,Z} + E^{\rm K}_{A,Z}(T) + E^*_{A,Z}(T) + E^{\rm C}_{A,Z}. \tag{4}$$

The contributions to the fragment energy $E_{A,Z}(T)$ on the right side of the the equation are the binding energy $B_{A,Z}$, the translational motion $E^{\rm K}_{A,Z}(T)$, the internal excitation energy $E^*_{A,Z}(T)$, and the remaining Coulomb terms $E^{\rm C}_{A,Z}(V)$, respectively. In all of the calculations, we use the Liquid Drop formula adopted in Ref. [16],

$$B_{A,Z} = w_0 A - \beta_0 A^{2/3} - C_{\rm C}\frac{Z^2}{A^{1/3}} - K_{\rm asym}\frac{(A-2Z)^2}{A}\Bigg/\left[1+\frac{9}{4}\frac{K_{\rm asym}}{Q_{\rm asym}A^{1/3}}\right], \tag{5}$$

$$E^{\rm K}_{A,Z}(T) = \frac{3}{2}T, \tag{6}$$

$$E^*_{A,Z}(T) = \frac{T^2}{\epsilon_0}A + \left(\beta(T) - T\frac{{\rm d}\beta}{{\rm d}T} - \beta_0\right)A^{2/3}, \tag{7}$$

$$\beta(T) = \left[\frac{T_c^2 - T^2}{T_c^2 + T^2}\right]^{5/4}, \tag{8}$$

$$E^{\rm C}_{A,Z} = -C_{\rm C}\frac{Z^2}{A^{1/3}}\left(\frac{V_0}{V}\right)^{1/3}. \tag{9}$$

The parameters entering the above expression are $w_0 = 16.0$ MeV, $\beta_0 = 18.0$ MeV, $C_{\rm C} = 0.737$ MeV, $K_{\rm asym} = 30.0$ MeV, and $Q_{\rm asym} = 35.0$ MeV, $\epsilon_0 = 16.0$ MeV, and $T_{\rm c} = 16.0$ MeV is the critical temperature above which the surface contributions to the free energy and entropy vanish [21, 32].

The following section is devoted to calculating the free energy and entropy of the system composed of fragments of different partitions. The statistical weight ω_f of a fragmentation mode is calculated through the entropy,

$$\omega_f = \exp(S_f), \tag{10}$$

where S_f stands for the entropy, which is obtained from the sum of the contributions of each fragment associated with the mode f. It is related to the total energy and the Helmholtz free energy F through the standard thermodynamic expression.

The mean value of any physical observable $\langle O\rangle$ is obtained by weighing its value in each partition,

$$\langle O\rangle = \frac{\sum_f O_f \omega_f}{\sum_f \omega_f}. \tag{11}$$

The entropy S_f is calculated through the standard thermodynamical relation,

$$S = -\frac{{\rm d}F}{{\rm d}T}, \tag{12}$$

where

$$F = E - TS \tag{13}$$

is the Helmholtz free energy. For a fragmentation mode, f can be written as

$$F_{A,Z} = \sum_{A,Z} N_{A,Z}\left[-B_{A,Z} + f^*_{A,Z}(T) + f^{\rm trans}_{A,Z}(T)\right] + F_{\rm Coul}, \tag{14}$$

where the contributions from the fragment's translational motion $f^{\rm trans}_{A,Z}$ and internal excitation $f^*_{A,Z}$ are expressed as

$$f^{\rm trans}_{A,Z} = -T\left[\lg\left(\frac{g_{A,Z}V_f A^{3/2}}{\lambda_{\rm T}^3}\right) - \frac{\lg(N_{A,Z}!)}{N_{A,Z}}\right]. \tag{15}$$

$$f^*_{A,Z} = -\frac{T^2}{\epsilon_0}A + \beta_0 A^{2/3}\left[\left(\frac{T_c^2 - T^2}{T_c^2 + T^2}\right)^{5/4} - 1\right]. \quad (16)$$

In the above expression,

$$\lambda_T = \sqrt{\frac{2\pi\hbar^2}{m_n AT}}$$

is the thermal wavelength, m_n is the nucleon mass, $g_{A,Z}$ is the spin degeneracy factor, and V_f denotes the free volume. The quantity of binding energy $B_{A,Z}$ and the remaining Coulomb terms F_{Coul} are temperature independent and therefore correspond, respectively, to Eqs. (5) and (9).

In the formulation mentioned above, the total mass and charge of all fragments are supposed to be fixed by Eq. (1) and Eq. (2). These constraints are very important while dealing with finite nuclear systems, when fragment multiplicities are not too large. The energy conservation stated by Eq. (3) allows one to determine the microcanonical temperature T_f for each fragmentation mode *f*. Since it is very difficult to compute all of the fragmentation modes of a heavy source, the numerical procedure of generating the individual multifragmentation events was proposed on the basis of the Monte Carlo method [1, 9, 16, 17]. The main strategy of the model simulation consists of partitions within a certain multiplicity range, for which the statistical weight is large.

3 Results and discussions

In this section, the SMM model described within the microcanonical ensemble in the previous section is now applied to study the breakup of different excited nuclei systems. In order to investigate the isospin effect, we have calulated the $A_0 = 200$, $Z_0 = 78$ nucleus compared with $A_0 = 200$, $Z_0 = 100$ system, of which one is neutron rich nucleus and the other is a symmetric one. In this work, we keep the breakup volume fixed for all fragmentation modes and parametrize it through the expression $V_\chi = (1+\chi)V_0$, where V_0 denotes the volume of the system at normal density and $\chi \geqslant 0$ is an input parameter. We use $\chi = 2$ in all the calculations below.

First we consider the mean characteristics of a multifragment system, such as the average temperature and multiplicity. The caloric curves of the systems are displayed in Fig. 1. The average temperature as a function of the excitation energy shown in Fig. 1 is obtained in the microcanonical ensemble. The diomand-line is the average temperature curve of $A_0 = 200$, $Z_0 = 78$ nucleus, while the circle-line is the $A_0 = 200$, $Z_0 = 100$ system respectively. The values of the average temperature are about 1.9 MeV for the $Z_0 = 78$ nucleus and 2.3 MeV for $Z_0 = 100$ at $\varepsilon^* = 0.5$ MeV, and climb to 4.9 MeV at $\varepsilon^* = 5$ MeV. In both cases, the results clearly show that the temperature increases monotonously and the existence of a plateau in the caloric curve, which signals a liquid-gas phase transition, as is well known [33–36], if the breakup volume is kept fixed for all energies. We can also see from the figure that the curves change very little while the charge Z_0 changes from 78 to 100, which means that the temperature as a function of the excitation energy is a very stable variable of the multifragmentation model.

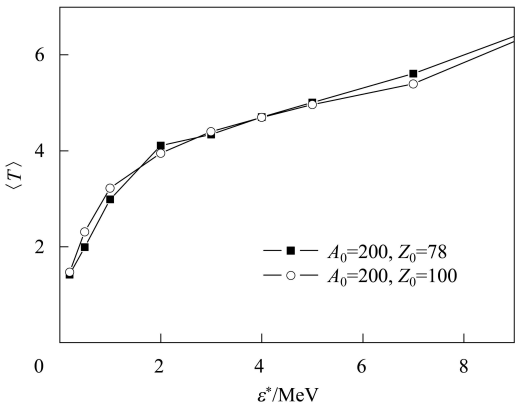

Fig. 1. The average temperature $\langle T\rangle$ of fragments versus the excitation energy in microcanonical calculation. The square-line is for the nucleus with $A_0 = 200$ and $Z_0 = 78$ while the circle-line for the $A_0 = 200, Z_0 = 100$ system.

In order to investigate the qualitative differences of the fragment multiplicity between the $A_0 = 200$, $Z_0 = 78$ and $A_0 = 200$, $Z_0 = 100$ systems, we show in Fig. 2 the average fragment multiplicity $\langle M\rangle$ as a function of the excitation energy. We can see that both curves increase monotonously with the growth in excitation energy. At the critical certain excitation energy ε^* at about 0.2 MeV/nucleon the fragmentation process sets in ($\langle M\rangle > 1$). Then the number of fragments grows rapidly and monotonously when the excitation energy gets higher. At $\varepsilon^* > 5$ MeV/nucleon the multiplicity $\langle M\rangle$ exceeds 10. It is important to note that when the excitation energy is lower than 1.0 MeV/u, the symmetric nucleus has larger multiplicity than the neutron-rich one, but drops down when the calculated excitation energy is higher than 1.0 MeV/u. For instance, at ε^*=7 MeV, $\langle M\rangle$ is increased by about 14.3% from 17.9 to 20.5, while the charge $Z_0 = 100$ changes to $Z_0 = 78$. This clearly

shows the isospin effect of the breakup fragment configuration, which means that the excited neutron-rich system ($Z_0 = 78$) has larger average multiplicity $\langle M \rangle$ at the higher excitation energy, and intends to break into more pieces with light nuclei.

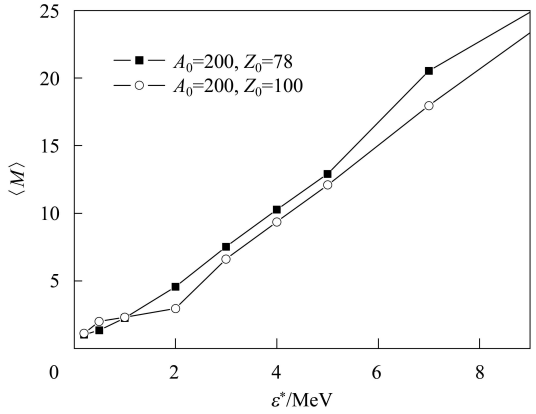

Fig. 2. The average multiplicity $\langle M \rangle$ of fragments versus the excitation energy for the two $A_0 = 200$ systems.

At lower excitation energies ($\varepsilon^* < 1.0$ MeV/u), the symmetric system's average temperature grows faster than the neutron-rich nucleus (shown in Fig. 1), and its average multiplicity is larger (shown in Fig. 2), which means an earlier beginning to the fragmentation process.

To further clarify the aspects discussed above, we now investigate the mass distributions predicted for the two different systems mentioned above. Fig. 3 and Fig. 4 show the average multiplicities N_A of fragments with mass A resulting from the break-up production. In Fig. 3, we can see that at lower excitation energy (ε^*=0.5 MeV), the mass distribution of the $Z_0 = 78$ system (solid-line) has a U-shape, which means that the dominating decay mode is "quasi-evaporation" (a break-up into a large residual nucleus and one or two light clusters). However, as the isospin effect is considered and we change the charge to $Z_0 = 100$, the mass distribution becomes a very different W-shape, which has a large probability of around $A_0/2$, which means that the disintegration mechanism has changed to "quasi-fission" (a break-up into two fragments with nearly equal masses and one or two light clusters). So we can say that the decaying mode of the symmetric system switches to a fission-like process from evaporation earlier than the neutron-rich nucleus at a lower excitation energy.

The mass distribution curves at a higher excitation energy $\varepsilon^* = 5$ MeV/u are also plotted in Fig. 4. We can see that they are both monotonically decreasing, and gradually approaching the exponential shape, but the largest fragment nucleus mass number still reaches about $A_0/2$, reflecting the liquid-gas coexistence of the break-up products.

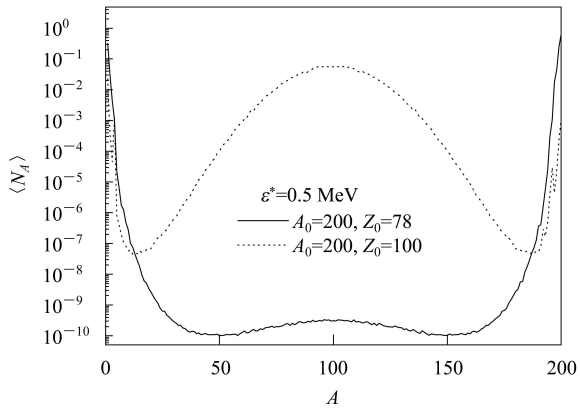

Fig. 3. The mass distributions of produced fragments predicted by the microcanonical ensemble at $\varepsilon^* = 0.5$ MeV/u. The solid and dashed lines are for the $A_0 = 200$, $Z_0 = 78$ and $A_0 = 200$ and $Z_0 = 100$ systems, respectively.

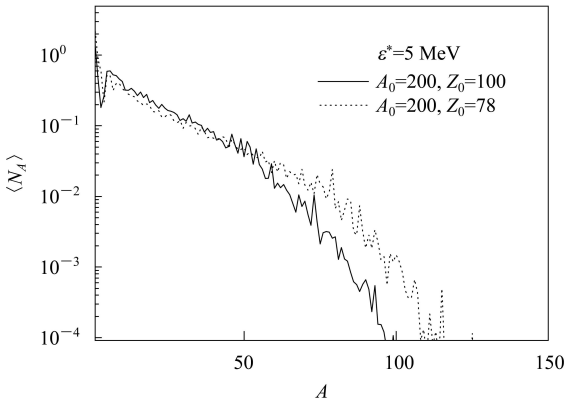

Fig. 4. The mass distributions of produced fragments calculated at $\varepsilon^* = 5$ MeV/u.

One can notice that the symmetric system ($Z_0 = 100$) has larger average multiplicities N_A of fragments in the medium-heavy nuclei range ($A \approx 10-40$), while the neutron-rich nucleus has a greater probability of breaking up with more lighter clusters and heavier residues, respectively, as discussed in Fig. 2.

4 Conclusion

In conclusion, the behavior of the nuclear caloric curves is investigated based on the statistical multifragmentation model within its micro-canonical ensemble. The average multiplicity and temperature sensitivities of the model as a function of excitation energy are discussed, and the mass distributions at two specific excitation energies ($\varepsilon^* = 0.5$ MeV/u and

$\varepsilon^* = 5$ MeV/u) are demonstrated. We concentrate on the isospin effect of the multifragmentation mechanism and the break-up fragment configuration by comparing the $A_0 = 200$, $Z_0 = 78$ and $A_0 = 200$, $Z_0 = 100$ systems. The calculations show that the break-up mode of the neutron-rich nucleus ($Z_0 = 78$) switches to a fission-like process from evaporation later than the symmetric system at lower excitation energies ($\varepsilon^* < 1.0$ MeV/u). While the excitation energy gets higher than 1.0 MeV/u, the neutron-rich nucleus has a larger average multiplicity $\langle M \rangle$ than the symmetric system at the same excitation energy, and intends to break into more pieces with light nuclei and heavier residues.

References

1 Dorf J, Botvina A S, Iljinov A S, MishustinI N. Phys. Rep., 1995, **257**: 133
2 Gross D H E. Rep. Prog. Phys., 1990, **53**: 605
3 PAN J, Gupta S D. Phys. Rev. C, 1995, **51**: 1384
4 Gupta S D, PAN J, Tsang M B. Phys. Rev. C, 1996, **54**: R2820
5 Bauer W. Phys. Rev. C, 1988, **38**: 1297
6 Pratt S, Montoya C, Ronning F. Phys. Lett. B, 1995, **349**: 261
7 Latora V, Belkacem M, Bonasera A. Phys. Rev. Lett., 1994, **73**: 1765
8 Gupta S D, Mekjian A Z. Phys. Rev. C, 1998, **57**: 1361
9 Botvina A S et al. Nucl. Phys. A, 1987, **475**: 663
10 Finn J E et al. Phys. Rev. Lett., 1982, **49**: 1321
11 Minich R W et al. Phys. Lett. B, 1982, **118**: 458
12 Hirsch A S et al. Phys. Rev. C, 1984, **29**: 508
13 Moretto L G, Wozniak G J et al. Rev. Nucl. Part. Sci., 1993, **43**: 379
14 Bondorf J P et al. Nucl. Phys. A, 1985, **443**: 321
15 Bondorf J P, Donangelo R, Mishusting I N. Nucl. Phys. A, 1985, **444**: 460
16 Sneppen K. Nucl. Phys. A, 1987, **470**: 213
17 Sneppen K, Donangelo R. Phys. Rev. C, 1989, **39**: 263
18 Bondorf J P et al. Phys. Lett. B, 1985, **150**: 57
19 Mishusin I N. Nucl. Phys. A, 1985, **447**: 67C
20 Barz H W, Bondorf J P, Donangelo R. Phys. Lett. B, 1986, **169**: 318
21 Barz H W, Bondorf J P, Donangelo R. Nucl. Phys. A, 1986, **448**: 753
22 Donangelo R, Sneppen K, Souza S R. Computer Physics Communications, 2001, **140**: 405
23 Gross D H E. Phys. Rep., 1997, **279**: 119
24 Henzlova D et al. Nucl. Part. Phys., 2010, **37**: 085010
25 Reuter P T, Bugaev K A. Phy. Lett. B, 2001, **517**: 233–238
26 Tsang M B, Gelbke C K X et al. Phys. Rev. C, 2001, **64**: 054615
27 Raduta A R, Gulminelli F. Phys. Rev. C, 2007, **75**: 024605
28 Bondorf J P, Botvina A S, Mishustin I N. Phys. Rev. C, 1998, **58**: R27
29 Aguiar C E, Donangelo R, Souza S R. Phys. Rev. C, 2006, **73**: 024613
30 Souza S R, Carlson B V, Donangelo R et al. Phys. Rev. C, 2009, **79**: 054602
31 Audi G, Wapstra A H. Nucl. Phys. A, 1995, **595**: 409
32 Souza S R, Danielewicz P, Gupta S D et al. Phys. Rev. C, 2003, **67**: R051602
33 Elliott J B, Hirsch A S. Phys. Rev. C, 2000, **61**: 054605
34 Chomaz P, Duflot V, Gulminelli F. Phys. Rev. Lett., 2000, **85**: 3587
35 Das C B, Gupta S D. Phys. Rev. C, 2003, **68**: 014607
36 Samaddar S K, de J N, Shlomo S. Phys. Rev. C, 2004, **69**: 064615